Evidence for in-plane antiferromagnetic domains in ultrathin NiO films

D. Spanke, V. Solinus, D. Knabben, and F. U. Hillebrecht
Institut für Angewandte Physik, Heinrich-Heine-Universität Düsseldorf, D-40225 Düsseldorf, Germany

F. Ciccacci
INFM, Dipartimento di Fisica, Politecnico di Milano, Piazza Leonardo da Vinci 32, I-20133 Milano, Italy

L. Gregoratti and M. Marsi
Syncrotrone di Trieste, Padriciano 99, I-34012 Trieste, Italy
(Received 23 February 1998)

Ultrathin films of NiO grown on Ag(100) were investigated by photoemission microscopy. To image antiferromagnetic domains, linearly polarized light from an insertion device was used. The micrographs revealed lateral changes of the spectral line shapes of the 3*p* photoemission spectrum which were confirmed by taking full spectra with a lateral resolution of 150 nm (microspectroscopy). These changes indicate the presence of antiferromagnetic domains which can be distinguished because the magnetic moments (or components thereof) are either collinear or perpendicular to the electric field vector of the linearly polarized light. [S0163-1829(98)01730-5]

The formation of magnetic domains is a common behavior of magnetically ordered materials. Though usually associated with ferromagnetic materials, where domain formation reduces the magnetostatic energy of a sample by reducing or avoiding large stray fields reaching out into the environment of the sample, domain formation occurs also in antiferromagnetic materials. As for ferromagnets, an antiferromagnetic domain is defined as a region in a crystal in which the pattern of magnetic moments is periodic in all three directions of space. An example is Cr, whose magnetic moments are parallel to the 100 directions, so that three different domains are possible. In the present study we address the case of NiO. For bulk material, magnetic moments are aligned ferromagnetically within 111 planes, with antiferromagnetic alignment of subsequent 111 planes. This leads to four different possible domains (*T* domains). Furthermore, there is a threefold axis in the 111 planes, which leads to three different domain types within each *T*-type domain. Considering also spin reversal, in principle 24 different domains are possible. Antiferromagnetic domain walls result either if there is a rotation of the direction of the moments within the ferromagnetic sheets (*S* walls) or if there is a change in crystallographic orientation of the ferromagnetic sheets (*T* walls).

Domains in antiferromagnets have recently been considered in the context of exchange biasing, which is used to modify the hysteresis loop of a thin ferromagnetic layer by exchange coupling to an antiferromagnetic layer.[1] The uncompensated spins of the antiferromagnet (AF) at the interface to the ferromagnetic (F) layer do not, or only to a small degree, experience the effect of the external field, so that the exchange coupling between the AF and F spins at the interface leads to a hysteresis loop shifted along the field axis. The observed exchange fields, i.e., the magnitude of the magnetic field shift, tend to be smaller than may be estimated from the number of spins and the coupling strength at the interface. Antiferromagnetic domains may be one cause for this discrepancy. Therefore experimental evidence on AF domains in ultrathin films is highly desirable.

In a ferromagnet the multidomain state can be characterized by a reduced or vanishing macroscopic magnetization. F domains are commonly detected by performing a spatially resolved experiment which reveals contrast due to the nonvanishing *local* magnetization. These methods do not work for AF domains where also the local magnetization vanishes. Observations of AF domain ordering in transition metal monoxides have been made by neutron- and x-ray-scattering methods as well as linear birefringence.[2–4] The two latter methods in principle depend on the lattice distortion incurred by AF order. Below T_N the antiferromagnetic ordering results in a slight rhombohedral deformation of the crystal, which comes about by a contraction of the original cubic unit cell along the 111 axes: In the AF ordered state the spacing between subsequent AF aligned ferromagnetic planes is reduced. A domain can be considered as an optical uniaxial crystal, with the optical axis coincident with the axis of contraction. Different domains and walls between them can be made visible in 100 μm thin crystal by transmitted polarized light. The crystallographic distortion can also be detected directly by x-ray diffraction. For ultrathin films these methods are difficult to use because it is not clear to which degree surface and/or interface anisotropies will lead to a differently ordered AF state compared to the bulk.

We report here an attempt to investigate the spin orientation in ultrathin NiO films directly in a spatially resolved way by exploiting linear magnetic dichroism in photoemission. Linear dichroism in general requires no net magnetization, but may show up in terms of different optical or spectral properties depending on whether the polarization vector of the light is parallel or perpendicular to the preferred spin orientation. In photoemission, this type of dichroism has been observed for the Fe 3*p* spectrum,[5] and calculations exist for other materials.[6] Photoabsorption experiments on ultrathin NiO films have been reported by Vogel[7] and Alders

et al.[8–10] Here, a preferred spin axis was imposed by thin film epitaxial growth on MgO(100) single crystal substrates. From a detailed analysis of the *2p* absorption edges it was concluded that in such thin film samples only domains with spin directions $[\pm 2, \pm 1, \pm 1]$ were present. The experimental line shape for the $2p_{1/2}$ absorption edge consists of two peaks, separated by about 1.5 eV, and under normal incidence the lower-energy peak is higher than the higher-energy one if only domains of this subset are present. Angle-dependent studies showed a reversal of this intensity relation for grazing incidence, where the spin moments have a large projection on the electric field vector of the incoming light.[7,9]

The experiments reported here were performed on the ESCA Microscopy beamline[11,12] at the ELETTRA synchrotron radiation source in Trieste, Italy. The light emitted by a 4.5 m, 56 mm period undulator is dispersed by a spherical grating monochromator in the 200–1000 eV photon energy range. This beam is focused by a Fresnel zone plate to a microspot of about 120–150 nm diameter. The specimen is mounted on a piezodriven scanning stage, which provides movement of the sample with respect to the photon beam. A 100 mm mean radius hemispherical analyzer, equipped with multichannel detection, collects the photoelectrons emitted from the microspot, with an overall energy resolution of 0.3–0.5 eV. Because of the photon energy dependence of the zone plate focal length, refocusing is required when the photon energy is changed. However, during the acquisition of the absorption spectra, the zone-plate–sample distance was not changed, because the change in focal distance is negligibly small for the energy interval of interest.

The present study was performed on NiO films grown in a UHV chamber connected to the microscope equipped with low-energy electron diffraction (LEED) and Auger spectroscopy on Ag(100) single crystal surfaces as described by Marre *et al.*[13,14] The lattice constant of Ag is smaller than that of NiO by 2.05%, which allows for good epitaxial growth of NiO on Ag(100). Prior to deposition, the Ag crystal surfaces were cleaned by sputtering and annealing, and exhibited a high contrast LEED pattern. Sample cleanliness was checked by Auger spectroscopy. Ni was evaporated by electron beam heating of a Ni rod. Calibration of the evaporation rate by taking a series of Auger spectra yielded a value of about 0.8 monolayers Ni per minute. For growing NiO films, an O_2 pressure of 10^{-6} mbar was established in the deposition chamber before starting deposition (with the evaporator in operation, but the shutter closed). During deposition the sample was at room temperature. The films showed a LEED pattern similar to those of the substrate crystals, and Auger spectra showed only Ni and O in a ratio consistent with NiO. For the experiments reported here the azimuthal orientation of the Ag crystal was such that the electric field vector of the linearly polarized light was parallel to a [011] direction in the Ag(100) surface. As a discriminative criterion for the formation of NiO we use the valence band photoemission spectrum, which is displayed in Fig. 1(a). This figure shows all the features characteristic for NiO: A large narrow peak of primarily Ni *d* character at 2.3 eV binding energy (BE), a broad band of mixed Ni *d*-O *p* character extending to about 13 eV BE, and finally the O 2*s* emission feature 22 eV BE.[15,16] Comparison to a metallic sample

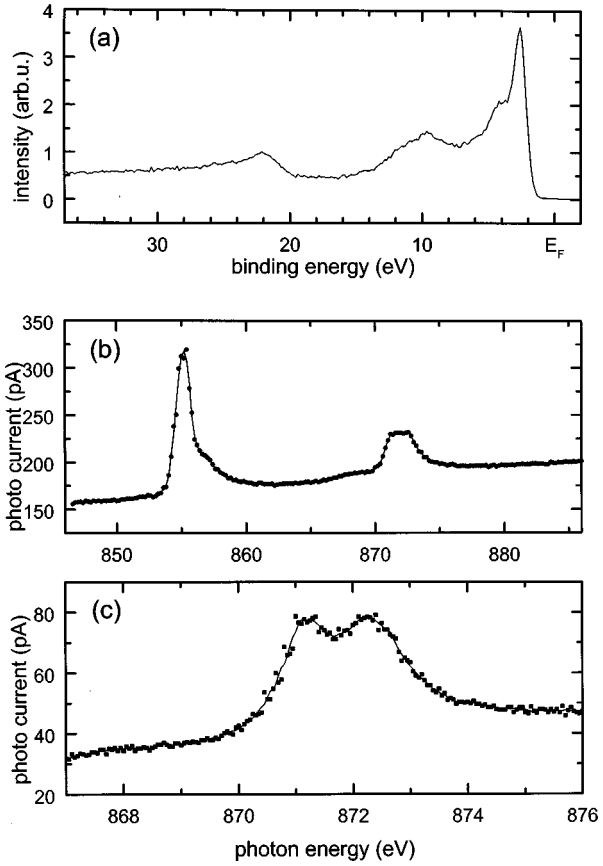

FIG. 1. (a) Photoemission spectrum of the valence band and shallow core levels of NiO grown on Ag(100), taken with 497 eV linearly polarized photons under normal incidence; emission was 70° to the surface normal, (b) Ni 2*p* absorption spectrum for NiO grown on Ag(100), taken with a large (200 μm) light beam diameter. (c) Detail of Ni $2p_{1/2}$ absorption spectrum.

shows that the onset of the emission is below the Fermi level, demonstrating the absence of metallic Ni or Ag species.

Another criterion for the formation of NiO is the Ni 2*p* absorption spectrum shown in Fig. 1(b), which also exhibits the characteristic features of NiO, a so-called white line with a satellite at the $2p_{3/2}$ edge and a double peak at the $2p_{1/2}$ threshold. Figure 1(c) shows an absorption spectrum of the $2p_{1/2}$ edge under normal incidence. We note that the higher-energy feature has about the same intensity as the lower-energy one. This is in contrast to the results obtained by Alders *et al.*[9] in normal incidence measurements on films grown on MgO.

The aim of the microscopy experiments was to investigate whether photoemission or absorption spectra obtained from small areas show changes with lateral position which would indicate different orientations of the magnetic moments. We first used the contrast mechanism described above for photoemission. In those experiments, the Fe 3*p* photoemission spectrum was found to be different depending on whether the electric field vector of the light was parallel or perpendicular to the orientation of the magnetic moments.[5] Reversal of the magnetization does not affect the spectrum. The dichroism, i.e., the difference of the spectra normalized to the sum, shows for the case of Fe a characteristic W-like shape. As became apparent from calculations, this comes about be-

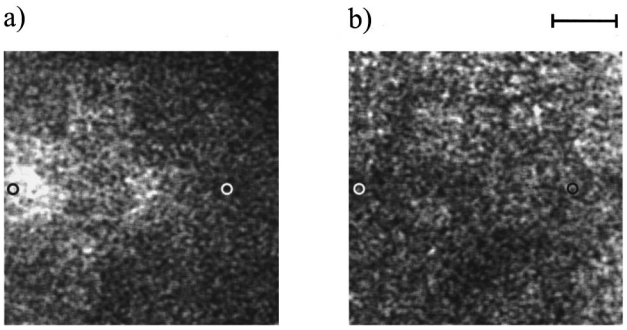

FIG. 2. Photoemission images taken with different portions of the Ni 3*p* photoemission spectrum excited by 497 eV linearly polarized photons: (a) binding energy $E_B = 67.2$ eV; (b) $E_B = 69.5$ eV. The scale bar represents a length of 15 μm. Circles show areas used for photoelectron intensity determination for various kinetic energies (see Fig. 3).

cause emission from the $m_j = \pm\frac{3}{2}$ sublevels which appears at the upper and lower edges of the $j = \frac{3}{2}$ multiplet, have different intensities than the $m_j = \pm\frac{1}{2}$ sublevels which appear with intermediate binding energy.[17–19] In the simplest approach, one assumes that the main effect of the incompletely filled *3d* shell is to split the m_j levels in a Zeeman-like fashion.[17,18] The $j = \frac{1}{2}$ sublevel does not show any or only a small[19] dichroism. While this picture seems to capture the essential features for metallic systems, the situation for NiO is obviously not well described since all core level spectra show distinct satellites.[16] Nevertheless, referring to the calculation by Thole and van der Laan[6] for a d^8 system as a starting point, one may anticipate that the largest effect of the linear magnetic dichroism of domain imaging to be used occurs on the low binding energy side of the *3p* photoemission spectrum.

We acquired photoelectron intensity images of various regions on the sample using light focused to a spot of about 150 nm. The images consisted of 256×256 pixels which covered an area of 64×64 μm^2. The photon energy was set to 497 eV. At the time of the experiment, image acquisition in the photoemission microscopy mode was performed by measuring the count rate of the spectrometer as pixel intensity while scanning the sample using the piezodrives. With the pass energy used, the energy resolution was about 1.5 eV. The kinetic energy was set to different values, covering the Ni 3*p* photoemission peak. Figure 2(a) shows the photoemission image obtained with 429.8 eV kinetic energy photoelectrons (67.2 eV binding energy E_B).One can see a bright area in the middle on the left of the image. Figure 2(b) shows an image of the same area, but now acquired using photoelectrons with binding energy $E_B = 69.5$ eV. Here, the same area appears dark, while the region in the upper right corner is now brighter than in the previous image. We ascribe this to different preferential spin orientations in the sample, i.e., to different domains.

Figure 3 shows full photoemission spectra taken with a small light spot in different regions of the image of Fig. 2. Spectra were taken in the bright (middle left) and dark (upper right) regions of Fig. 2(a). The spectra and the normalized difference (asymmetry) are shown in Figs. 3(a) and 3(b), respectively. One can clearly see a difference at the high-energy flank of the Ni 3*p* photoemission peak. In addition,

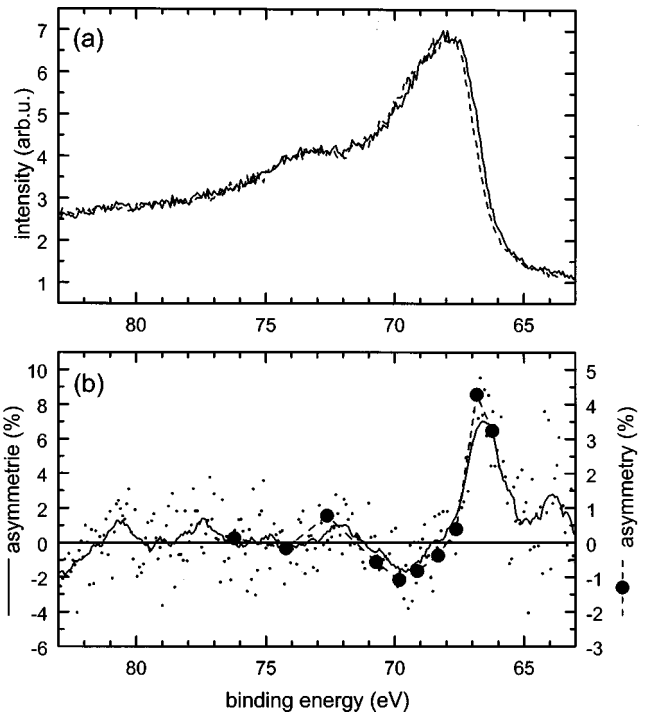

FIG. 3. Ni 3*p* photoemission spectra from different regions of the micrograph of Fig. 2 (marked with circles). Spectra shown in full and dashed were taken on the middle left and right region of the sample, respectively. (b) Asymmetry derived from spectra in (a) (small dots and full line representing a spline fit), and from intensities of the two regions in a series of images obtained with different kinetic energy photoelectrons (large dots and dashed line).

Fig. 3(b) shows a difference spectrum extracted from a series of images (filled circles) taken with different binding energies over the 3*p* spectrum by integrating over areas at the middle left and upper right. This spectrum is similar to the dichroism spectrum derived from the full spectra, even though the magnitude of the dichroism is smaller in the data derived from the series of images. This is consistent with the better energy resolution achieved in the spectra compared to the imaging.

Additional evidence for the presence of AF domains is derived from absorption spectra (measured by total yield) from different 150 nm spots on the sample which are presented in Fig. 4. The area analyzed here cannot be related to the area of the photoemission micrographs in Fig. 2, since the sample had to be removed from the beam for focusing at 870 eV photon energy. Figure 4 shows that spectra from different spots have a different intensity ratio of the low to the high photon energy absorption features at 871 and 872.3 eV. This difference is qualitatively similar to the dichroism expected for the light polarization being either parallel or perpendicular to the magnetic moments.[9] The magnitude of the dichroism, however, appears to be smaller than that observed by Alders *et al.*[9] The presence of different *T* domains within the spot of 150 nm appears unlikely since this size is of the order of domain wall thickness which is expected to be larger than for ferromagnets.[20] The reduced dichroism may be caused by the finite film thickness of 16 monolayers[21] of our sample which lowers the Néel temperature, and therefore leads to a reduced magnetic moment at room temperature.

The experimental results show that different regions on

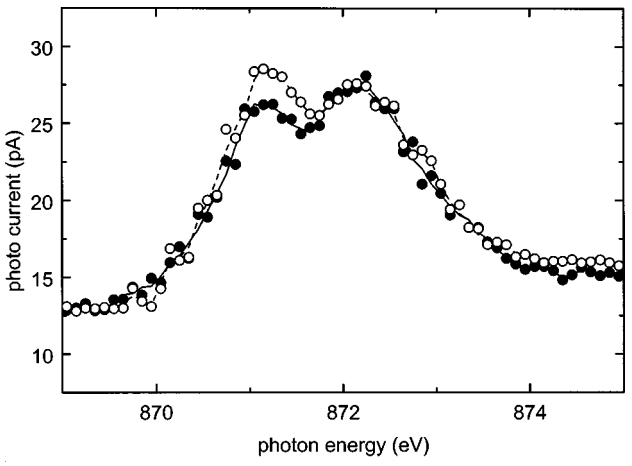

FIG. 4. Detail of the Ni $2p_{1/2}$ absorption at two different spots of ~150 nm diameter on the sample.

the sample are different with respect to the magnitude of the projection of the magnetic moments on the direction of the electric field vector. As the electric field vector was parallel to the in-plane [011] direction, the observed contrast is consistent with the subset of domains suggested for NiO/MgO. One type of spectrum would then correspond to domains with spin directions $[\pm 2,1,1]/[\pm 2,-1,-1]$, the other to $[\pm 2,-1,1]/[\pm 2,1,-1]$. Our experiment does not provide direct evidence on the magnitude of the projection on the surface normal, i.e., we cannot rule out that the moments lie in the sample plane, corresponding to directions [0,1,1], etc. In principle this could be determined from the magnitude of the dichroism, or more directly from angle-dependent measurements which are not possible in the microscope due to the short distance from the zone plate optics to the sample.

The orientation of the magnetic moments can be inferred from the fact that a dichroism is seen in this particular orientation. The azimuthal orientation of the Ag crystal was such that its 110 direction, and consequently the 110 direction of the NiO film within the film plane was parallel to the electric field of the incoming light. If the preferred direction of the magnetic moments was the 100 direction, then there would be no contrast between different domains, since both differently oriented domains would have the same projection of the magnetic moments on the direction parallel and perpendicular to the light polarization.

In summary, we have shown by photoemission microscopy combined with highly spatially resolved spectroscopic experiments that antiferromagnetic domains can be observed in thin (100)-oriented NiO films. They have a preferential orientation of the magnetic moments along the [110] directions within the film plane. This deviation from the orientation of the magnetic moments observed in bulk material is probably due the combined influence of surface anisotropy and the structural mismatch between substrate and film. Linear magnetic dichroism in photoemission as well as in photoabsorption appears to be a very powerful tool for the investigation of antiferromagnetic thin films with respect to ordering temperature, anisotropy, and the dependence of these properties on film thickness and morphology.

We thank E. Kisker for his continuous support. This work was supported by BMBF under Grant Nos. 05 621 PFA 7 and 05 644 PFA 1 and by Deutsche Forschungsgemeinschaft (DFG) within Grant No. SFB 166/G7.

[1] P. A. A. van der Heijden, T. F. M. M. Maas, W. J. M. de Jonge, J. C. S. Kools, F. Roozeboom, and P. J. van der Zaag, Appl. Phys. Lett. **72**, 492 (1998).
[2] W. L. Roth, J. Appl. Phys. **31**, 2000 (1960).
[3] T. Yamada, J. Phys. Soc. Jpn. **21**, 650 (1966).
[4] H. Kondoh and T. Takeda, J. Phys. Soc. Jpn. **19**, 2041 (1964).
[5] Ch. Roth, H. B. Rose, F. U. Hillebrecht, and E. Kisker, Solid State Commun. **86**, 647 (1993).
[6] B. T. Thole and G. van der Laan, Phys. Rev. Lett. **67**, 3306 (1991); Phys. Rev. B **44**, 12 424 (1991).
[7] Jan Vogel, Ph.D. thesis, Nijmegen, 1994.
[8] Dennis Alders, Ph.D. thesis, Groningen, 1996.
[9] D. Alders, J. Vogel, C. Levelut, S. D. Peacor, T. Hibma, M. Sacchi, L. H. Tjeng, C. T. Chen, G. van der Laan, B. T. Thole, and G. A. Sawatzky, Europhys. Lett. **32**, 259 (1995).
[10] D. Alders, T. Hibma, G. A. Sawatzky, K. C. Cheung, G. E. van Dorssen, H. A. Padmore, M. D. Roper, G. van der Laan, J. Vogel, and M. Sacchi, J. Appl. Phys. **82**, 3120 (1997).
[11] L. Casalis, W. Jark, M. Kiskinova, D. Lonza, P. Melpignano, D. Morris, R. Rosei, A. Savoia, A. Abrami, C. Fava, P. Furlan, R. Pugliese, D. Vivoda, G. Sandrin, F.-Q. Wei, S. Contarini, L. DeAngelis, C. Cariazzo, P. Nataletti, and G. R. Morrison, Rev. Sci. Instrum. **66**, 4870 (1995).
[12] M. Marsi, L. Casalis, L. Gregoratti, S. Günther, A. Kolmakov, J. Kovac, D. Lonza, and M. Kiskonova, J. Electron Spectrosc. Relat. Phenom. **84**, 73 (1997).
[13] K. Marre, H. Neddermeyer, A. Chassé, and P. Rennert, Surf. Sci. **357-38**, 233 (1996).
[14] Th. Bertrams and H. Neddermeyer, J. Vac. Sci. Technol. B **14**, 1141 (1996).
[15] J. Zaanen, G. A. Sawatzky, and J. W. Allen, J. Magn. Magn. Mater. **54-57**, 607 (1986).
[16] C. Scharfschwerdt, T. Liedtke, M. Neumann, T. Straub, and P. Steiner, Phys. Rev. B **48**, 6919 (1993).
[17] N. A. Cherepkov, Phys. Rev. B **50**, 13 813 (1994).
[18] Ch. A. R. Roth, J. Magn. Magn. Mater. **148**, 58 (1995).
[19] G. van der Laan, J. Magn. Magn. Mater. **148**, 53 (1995), Figs. 4 and 5.
[20] A. Hubert, *Theorie der Domänenwände in Geordneten Materialien* (Springer, Berlin, 1974).
[21] D. Alders (see Ref. 8) reports $T_N = 430$ K for 10 monolayers and 470 K for 20 monolayers. We estimate $T_N = 450$ K for 16 monolayers.